NOAA Technical Memorandum NWS SR-198

A METEOROLOGICAL AND RADAR ANALYSIS OF THE CENTRAL TEXAS TORNADO OUTBREAK ON MAY 27, 1997

Carl Morgan, Jeff Orrock, Nezette Rydell, and Jimmy Ward
National Weather Service Office
Austin/San Antonio, Texas

Scientific Services Division
Southern Region
Fort Worth, TX

July 1998

UNITED STATES
DEPARTMENT OF COMMERCE
William M. Daley, Secretary

National Oceanic and Atmospheric Administration
D. James Baker
Under Secretary and Administrator

National Weather Service
John J. Kelly, Jr.
Assistant Administrator
for Weather Services

1. INTRODUCTION

A severe weather event exploded across central Texas during the afternoon and evening hours of May 27, 1997. Supercell storms that developed in the extremely unstable airmass spawned numerous tornadoes, dropped large hail and produced damaging surface winds. Three strong tornadoes (F5, F3 and F4 damage intensity) were the cause of 28 fatalities and several million dollars in damages across two counties encompassing the Austin metropolitan area. This paper examines the pre-storm environment and radar observations of the event.

2. PRE-STORM SYNOPTIC ENVIRONMENT

a. Early Morning Environment

During the 12-24 hours preceding the severe weather outbreak, the large scale synoptic environment was evolving into an extremely unstable regime. The general upper-air pattern on the morning of May 27 indicated a broad 500 mb trough across the central plains states. A small jet streak at 300 mb was positioned so that Texas was in the right entrance (rear) region of the streak.

At the surface (Fig. 1) a cold front, associated with the 500 mb vorticity field, stretched from a surface low in Arkansas southwestward into north central and southwest Texas. Convection which had moved across portions of Oklahoma and Arkansas was dissipating in eastern Arkansas. An associated outflow boundary arched across the southern portion of Arkansas into the Arklatex region.

Convective Available Potential Energy (CAPE) values were around 5000 JKg^{-1} at Del Rio with an axis near 4000 JKg^{-1} northeastward into north central Texas. The 1200 UTC radiosonde sounding for Del Rio, Texas (Fig. 2), located along the Texas-Mexican border in Southwest Texas indicated abundant low-level moisture, and a near adiabatic lapse rate in the lower half of the atmosphere. This sounding appeared to be representative of the air mass eastward and northeastward of Del Rio, into central Texas where the severe weather event in this discussion developed.

A gravity wave, quite evident on visible satellite animation and apparently generated by the collapsing convection and outflow boundary, was spreading rapidly southward across northeast Texas and northern Louisiana. The western edge of this gravity wave would move southwestward along the cold front in north central and central Texas. An axis of moisture flux convergence near the surface stretched along and just to the east and south of the cold front, with highest values across north central Texas.

b. Early Afternoon Environment.

By 1800 UTC (1 pm CDT, or about the time strong convection was developing near central Texas) the 6-hr ETA 300 mb map continued to show a 70-kt jet streak from southwest to northeast across Missouri and Oklahoma. At 500 mb the broad trough continued across the eastern Rocky Mountains into the southern Plains. An embedded short wave was shown back across Colorado and New Mexico, likely too far west to significantly affect central Texas during the midday. Overall, the dynamics were not strong, but would not be inhibiting convection.

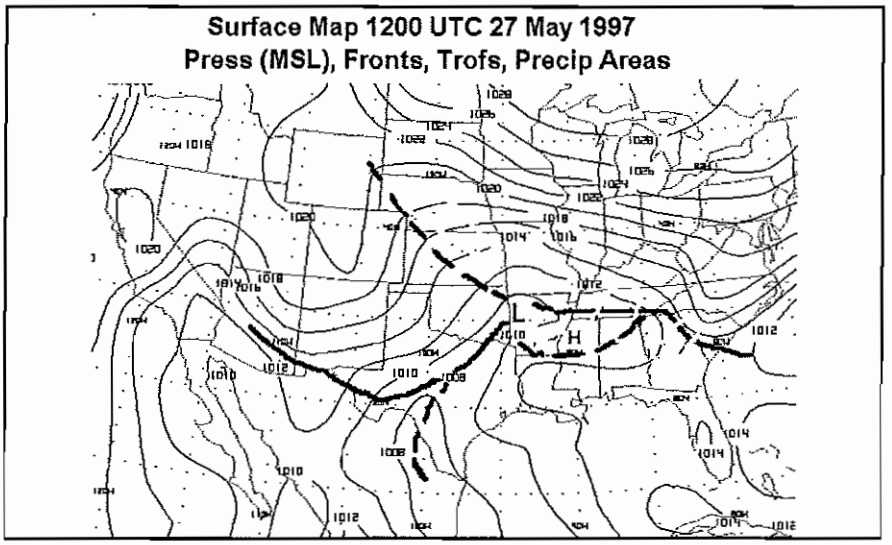

Figure 1

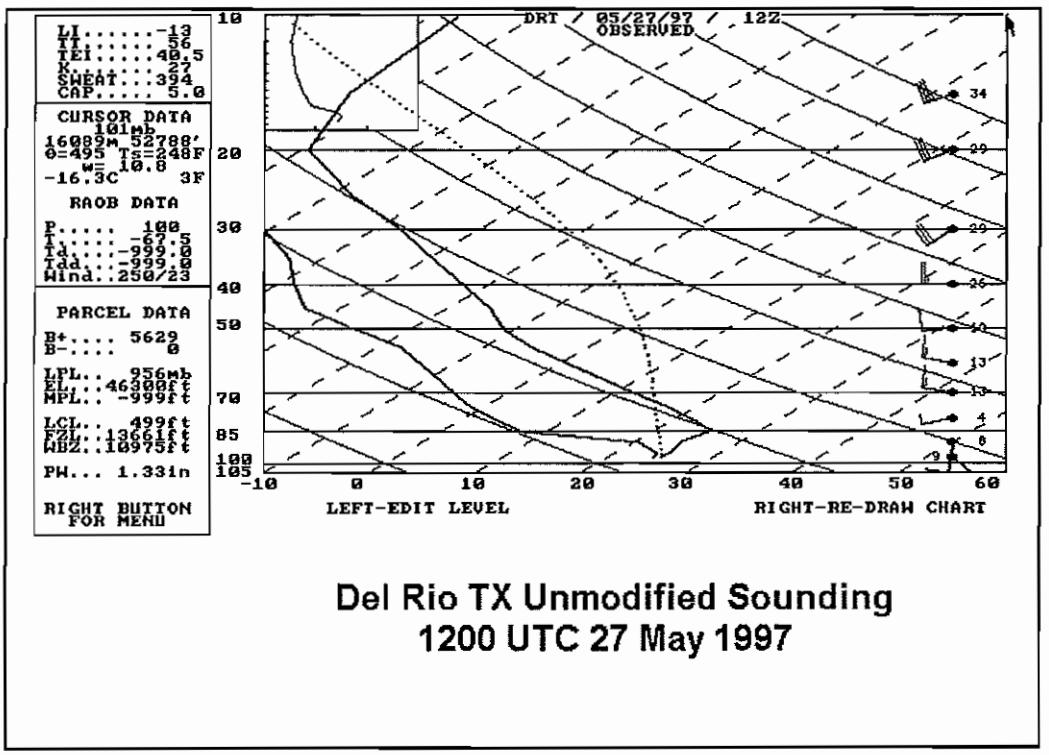

Figure 2

Moisture flux convergence on the 6-hr ETA model showed a strong maximum in central Texas. The axis of 850 mb Theta-e extended from Del Rio into central Texas (Fig. 3). The CAPE values were forecast to be 5000+ JKg^{-1} in central Texas from southwest of San Antonio northeastward across the Austin and Temple area.

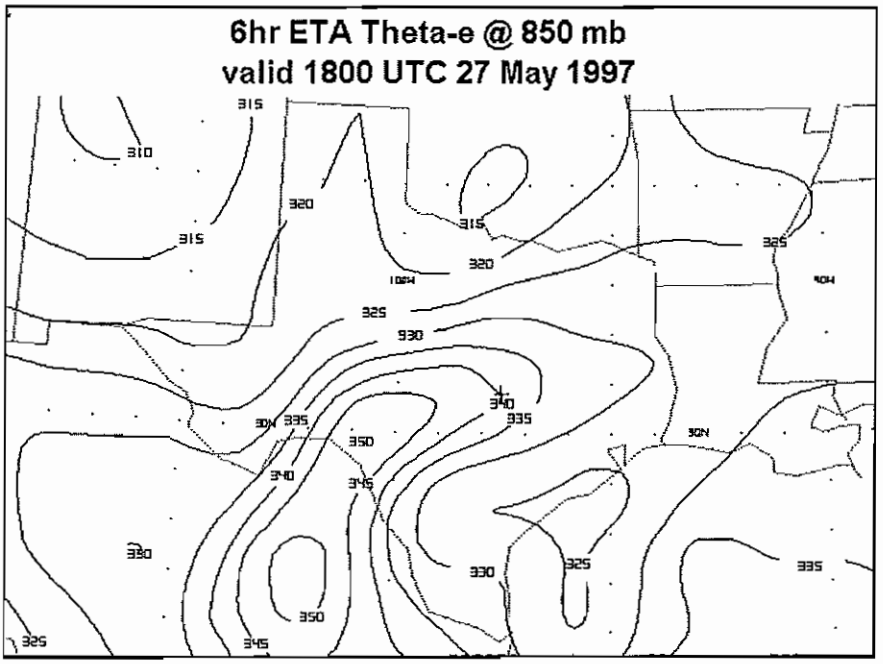

Figure 3

The weak, nearly stationary frontal boundary lay across central Texas during the early afternoon hours. The boundary was clearly visible on satellite imagery as a line of cumulus clouds extended from Del Rio to near Temple and Waco. Dew points were in the lower to middle 70s from the boundary southeastward to the Texas coast. Drier air lay behind the boundary where dew points were in the lower 60s. Lifted index values were -13 °C. Wind profiles from the soundings as well as from local WSR-88Ds through the morning hours indicated only light winds near the surface and little or no shear through 6 km.

The gravity wave mentioned earlier moved rapidly southward along the frontal boundary in north central Texas during midday. As the gravity wave crossed the counties around Waco, convection which had just begun to develop with heating along the frontal boundary, strengthened very rapidly during the early afternoon hours (Fig. 4).

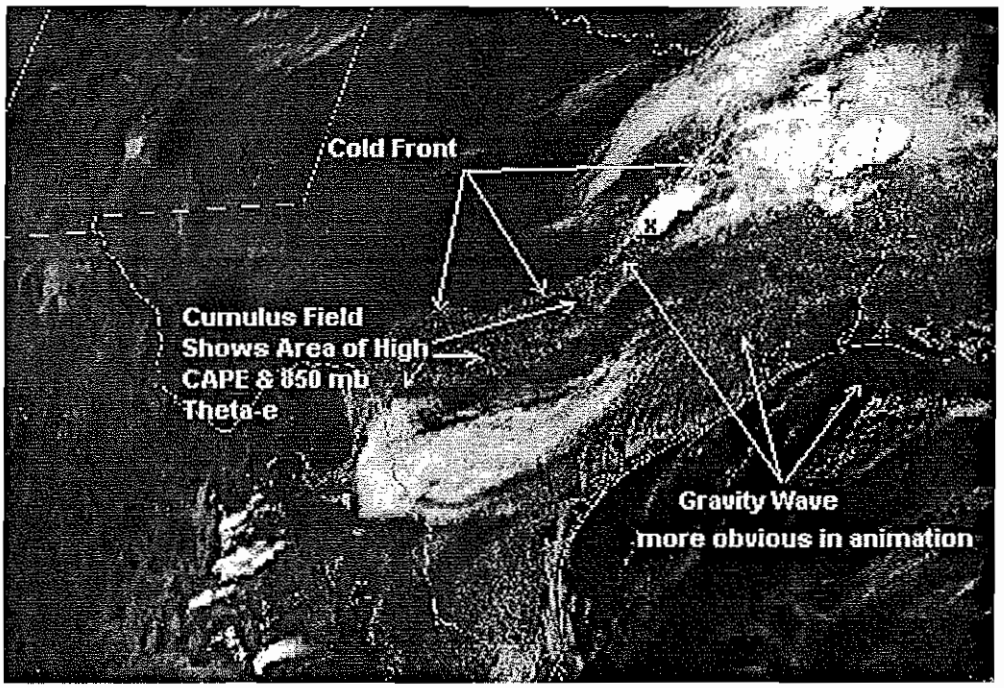

Figure 4. Early afternoon features depicted on the visible satellite imagery. "X" indicates the beginning of the significant convection.

3. MESOSCALE STORM-RELATIVE ENVIRONMENT

a. Unmodified Environment Near Storm Initiation

The morning sounding from Del Rio as discussed previously revealed that an extremely unstable airmass was in place south of the frontal boundary. Unmodified, the Del Rio sounding produced a CAPE of 5629 JKg^{-1} and a lifted index of -13 °C. Also revealed was a relatively weak environmental wind field. The 0-6 km ground-relative mean wind was from 250 degrees at 6 knots, and the SHARP PC program yielded a 0-3 km storm-relative helicity of -27 m^2s^{-2}.

b. Modified Storm Environment

Modifications were made to the Del Rio sounding to accommodate daytime heating, both at the surface, and in the lower and mid-levels of the dry air aloft. The resulting CAPE value increased to 6725 JKg^{-1}, and the lifted index fell to -15 °C, reflecting an additional decrease in stability. The strong convection began to develop between 1700 UTC and 1800 UTC near Waco, at the intersection of the cold front and gravity wave.

As the thunderstorm developed, it propagated to the south-southwest along the cold front. This unusual storm motion appeared to be the result of the movement of the gravity wave, combined with a significant layer of north-northwest winds above 11,000 ft (as revealed by the VAD Wind Profile from the New Braunfels 88D Radar), and the available energy in the moist, unstable air to the south. The storms moved and regenerated along the surface boundary toward even greater unstable air.

With extremely large CAPE's, once a strong updraft was established and air parcels began to accelerate through the area of positive buoyancy, the storm inflow increased in a proportional manner. This effect was well documented by spotters. At a point 5 miles east of the storm, the peak ground-relative inflow was measured at 25-30 knots from the east-southeast. In addition to the enhanced storm inflow, the storm-relative winds above the inflow layer were more than double the magnitude of the ground-relative mean wind, due to the large component of the storm motion vector which opposed the mean wind. Combining the increased inflow with the unusual storm motion nearly 125° to the right of the mean wind, the storm-relative wind field took on a much more ominous character.

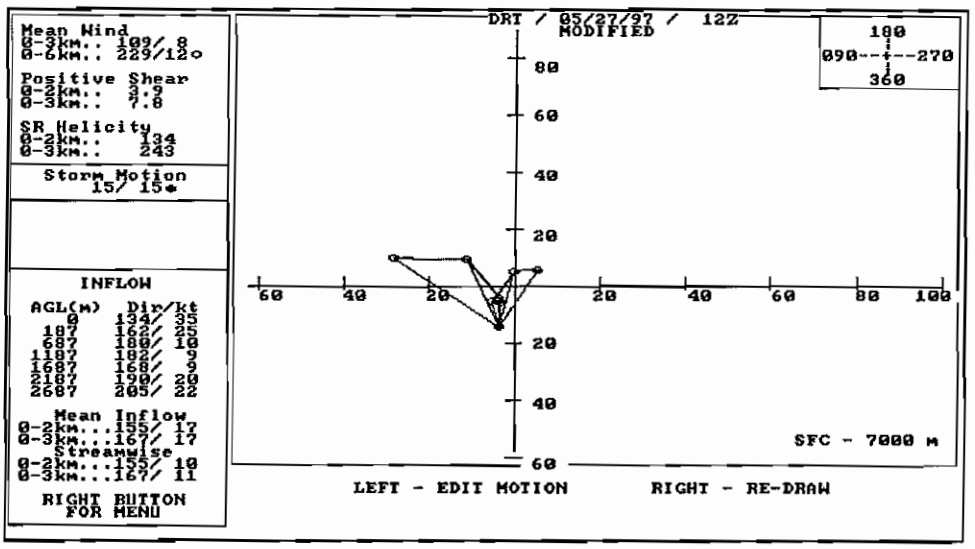

Figure 5. Modified Storm Environment Hodograph

Using a combination of the 1200 UTC sounding data from Del Rio, the VAD Wind Profile from New Braunfels, and surface-based reports from spotters, the SHARP program was used to generate a hodograph (Fig. 5) believed to be representative of the storm-relative wind field during the evolution of the supercell. SHARP, by default, calculates storm-relative helicity based on a storm motion vector 30° to the right of the 0-6 km mean wind, and at 75% of its magnitude. Storm motion in this case, however, was from approximately 15° at 15 knots.

c. Application of the Modified Helicity

After modifying the wind field to account for the enhanced storm inflow and observed storm motion, SHARP calculated a 0-3 km storm-relative helicity of 243 m^2s^{-2}. Davies-Jones, et al. (1990) suggested that when helicity values approach or exceed 150 m^2s^{-2}, then there is greater potential for mesocyclone-induced tornadoes, given adequate instability and forcing.

However, helicity alone can be a misleading value. Johns, et al. (1993) has shown that strong and violent tornadoes can and often do form in opposing extremes of helicity and instability. The Energy-Helicity Index (EHI) was developed by Hart and Korotky (1991) as a way to combine these parameters into one value for forecasting purposes. It is defined as EHI=CAPE(H)/160,000, where

H represents the 0-2 km storm-relative helicity.

Studies by Davies (1993) suggest that the following set of guidelines may be helpful when assessing the threat of supercell-induced tornadoes, assuming adequate support from storm-relative winds:

less than 2.0 -	significant mesocyclone-induced tornadoes unlikely
2.0 to 2.4 -	mesocyclone-induced tornadoes possible, but unlikely to be strong or long-lived
2.5 to 2.9 -	mesocyclone-induced tornadoes more likely
3.0 to 3.9 -	strong tornadoes (F3) possible
greater than 4.0 -	violent tornadoes (F4) possible

SHARP calculated the EHI from the Del Rio unmodified observed 1200 UTC sounding to be 0.88. When adjusted for the storm-relative parameters, this value increased significantly to 5.63 (Fig. 5).

May 27, 1997 presented a complex set of environmental parameters; extreme instability, a weak environmental wind field, and a slow-moving cold front intersected by a subtle outflow boundary. Although severe convection was anticipated, the family of violent tornadoes was not. The wind environment, unlike one normally associated with violent tornado outbreaks, was transformed by an unusual storm motion in an extremely unstable environment..

In a classic severe weather environment, strong vertical wind shear is needed to generate horizontal vorticity, which is then tilted into the vertical and stretched. Davies-Jones and Burgess (1990) note that environmental winds have little effect on storm structure when they are light in comparison to storm-induced winds. In this case, since strong wind shear was not a part of the pre-storm environment, the storm motion and inflow helped in creating the favorable wind field.

Storm motion, with a large component directed into the prevailing environmental wind, resulted in stronger storm-relative winds from the southwest, above the inflow layer. The final product was a storm-relative wind field which bore little or no resemblance to the environmental wind field, and was therefore able to help produce and sustain a family of violent tornadoes.

4. DESCRIPTION OF WSR-88D IMAGERY

a. The Jarrell Storm.

A relatively weak F0 to F1 tornado near Prairie Dell, in southern Bell county, tracked slowly southwestward into northern Williamson county, moving parallel and in close proximity to Interstate 35. This tornadic cell was propagating, more than moving, slowly southwestward along the frontal boundary.

At 2007 UTC, there were no radar echoes greater than 20 dBZ at the lowest elevation angles to the south or southwest of the tornadic supercell and no competition for inflow into the updraft. Reflectivity cross sections (Fig. 6) and composite reflectivity imagery (Fig. 7) showed development as much as 7 miles southwest of the tornadic supercell. New cells 16 miles to the southwest of the supercell were forming aloft between 20 and 30 kft.

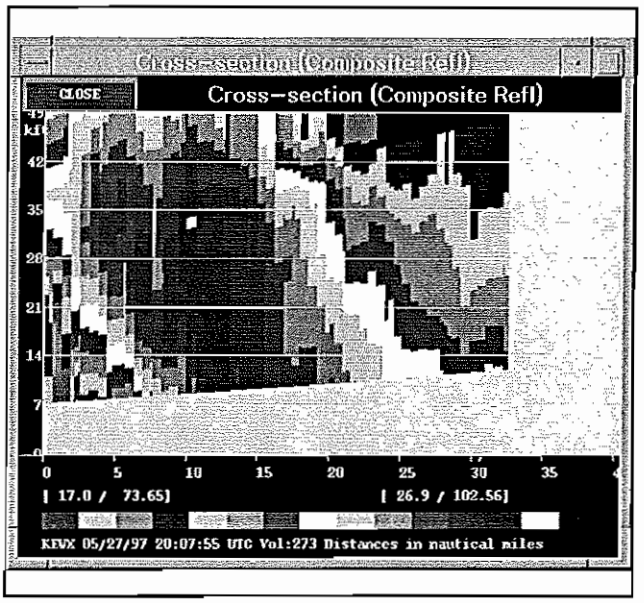

Figure 6. KEWX Reflectivity Cross Section (south to north) of storm at 2007 UTC .

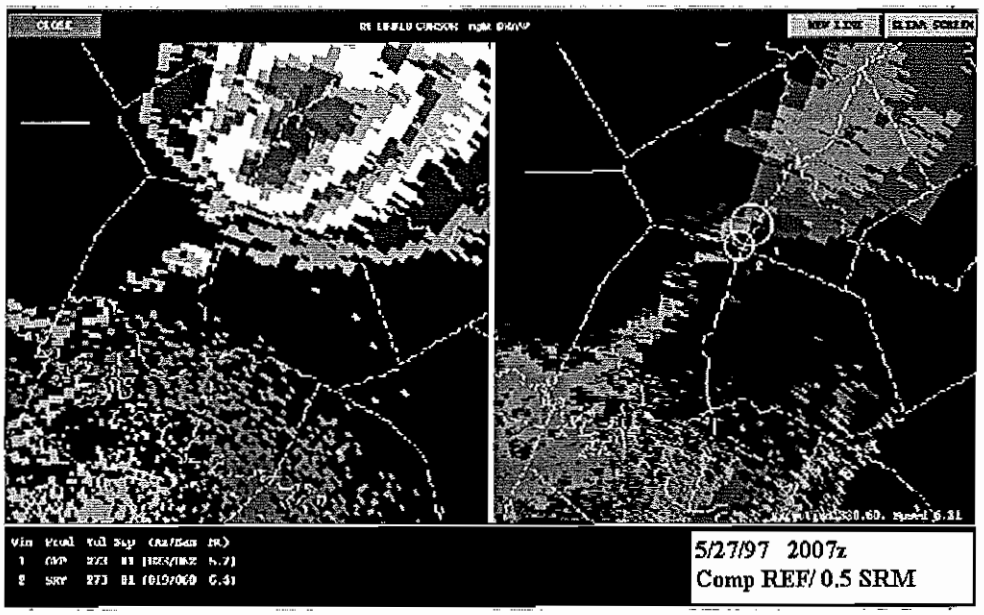

Figure 7. KEWX Composite Reflectivity (left) and 0.5° Storm Relative Velocity (right) at 2007 UTC.

At 2019 UTC (Fig. 8), the KEWX WSR-88D located 76 miles south of Jarrell measured 80 kts of gate-to-gate shear associated with the tornado in the low levels (about 7500 ft) in southern Bell county. The reflectivity cross section (Fig. 9) continued to show an impressive bounded weak echo region.

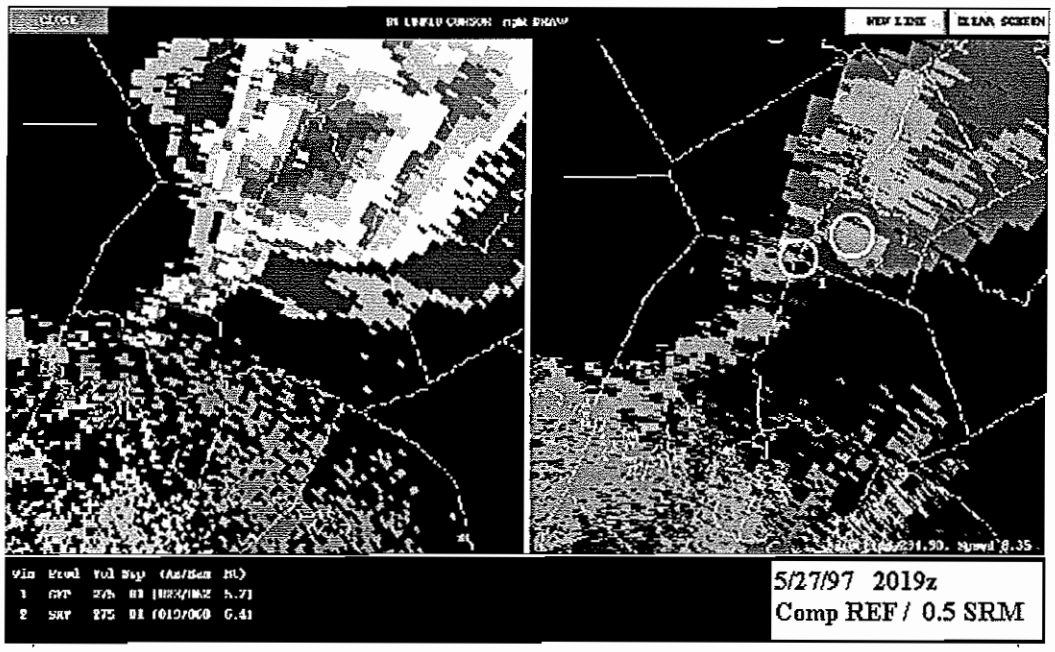

Figure 8. Composite Reflectivity (left) and Storm Relative Velocity at 0.5° Of the KEWX radar at 2019 UTC.

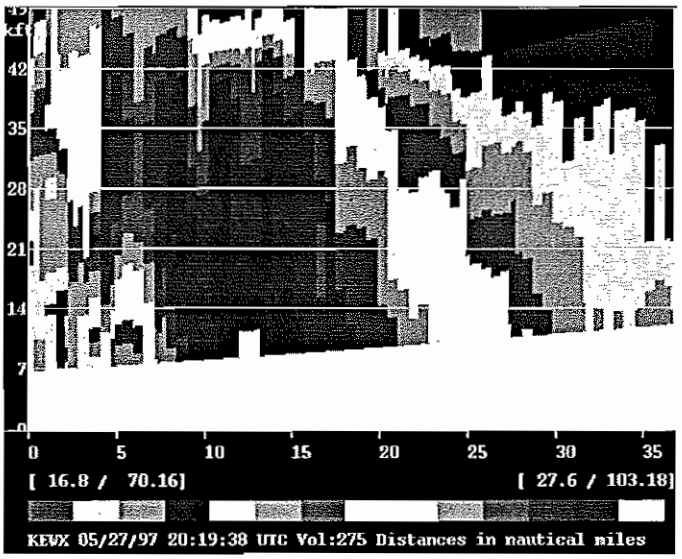

Figure 9. KEWX Reflectivity Cross Section at 2019 UTC.

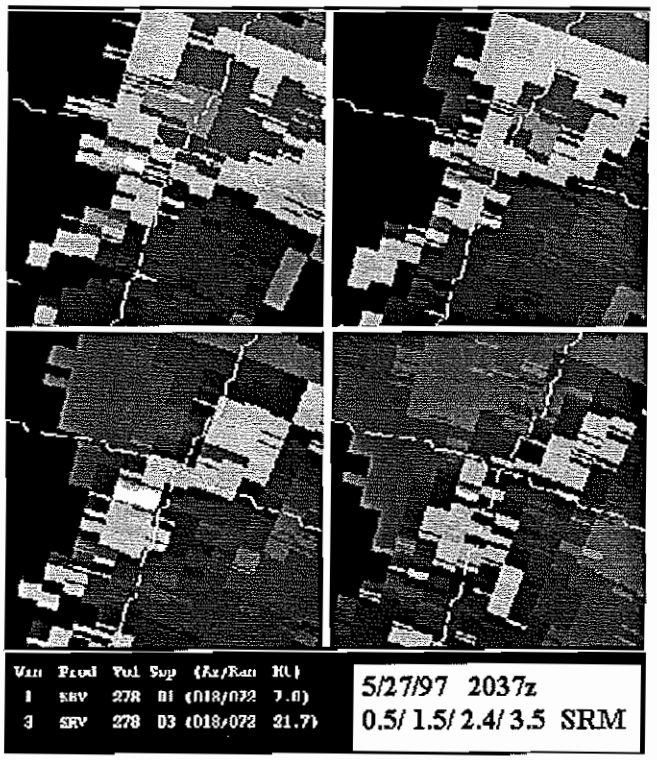

Figure 10. KEWX Storm Relative Velocity at 0.5°, 1.5°, 2.4°, 3.5° at 2037 UTC .

An F1-F2 tornado was on the ground at this time. A radar-defined mesocyclone was displaced slightly to the northeast of the operator-identified TVS. Base reflectivity images suggested a weak appendage on the southwest leading edge of the supercell. Storm relative velocities (SRM) from nearby KGRK at 2020 UTC showed an area of maximum rotation, as much as 110 kts of gate-to-gate shear, at the 4.3 and 6.0 degree elevation scans, approximately 7 to 10 kft. These high velocities were also evident on the KEWX SRM images from 2037 UTC to 2043 UTC at 15 to 20 kft.

Between 2035 UTC and 2040 UTC the main vortex descended to the surface creating a multi-vortex tornado that tracked southwestward toward Jarrell. Both the 2037 UTC (Fig. 10) and 2043 UTC SRM images at 0.5 and 1.5 degrees (Fig. 10) contain many pixels of "no data" (data dropout) in the vicinity of the highest rotational shear.

This loss of data, likely due to a pulse pair phase shift of greater than 180 degrees within the range bin, associated with a strong mesocyclone and/or suspected tornado is a strong indicator of tornadic activity (White, 1997). This phenomenon would reoccur later in the evening with a second tornado.

Figure 11. KEWX Storm Relative Velocity at 0.5°, 1.5°, 2.4°, 3.5° at 2043 UTC.

SRM products at 2043 UTC (Fig. 11) indicated 90 kts of gate-to-gate shear in a column spanning the lowest elevation scans from 0.5 degrees to 2.4 degrees, with many pixels of missing data in the area of highest velocity values. The F5 tornado was on the ground west of I-35 near Jarrell at this time.

Rapid development was occurring aloft and the mesocyclone and tornado vortex were well out ahead of the main core of the storm at a distance of some 8 miles. The tornado was on the ground within one volume scan of the time echos greater than 30 dBZ first appeared on the 0.5 degree reflectivity imagery at that location. The area of intense gate-to-gate shear, and the tornado itself, remained on the southwest leading edge of the 0.5 degree reflectivity imagery throughout the event. The missing velocity data in the lowest elevation scans of the SRM products before and during the tornado contributed to a failure of the mesocyclone detection algorithms and subsequently to the failure of the TVS algorithm.

The high resolution (.13 nm) spectrum width product used in conjunction with the velocity imagery located the mesocyclone/tornado vortex from the 2037 UTC through 2048 UTC volume scans. Various meteorological phenomena can cause high values of spectrum width (i.e. convergent zones, areas of turbulence, large hail, etc.). The radar depicted several other areas of high spectrum width in the same volume scans apart from those associated with the tornado. The coarser .54 nm resolution data did not conclusively locate the vortex.

By 2048 UTC, tornadic signatures in the radar velocity imagery had weakened. Spotter reports

indicated the tornado was dissipating at this time. Echos to the southwest, near Georgetown, were now apparent in the lowest elevation scan. These cells were producing large hail and funnel clouds. Further to the southwest along the boundary, very high reflectivities aloft were developing rapidly in southern Williamson County near the towns of Leander and Cedar park. Radar indicated a mesocyclone in this new cell.

b. The Cedar Park Storm.

Between 2106 UTC and 2118 UTC an F3 tornado tracked southwestward from near Leander to Cedar Park and into northern Travis county. On a larger scale (Fig. 12) the propagation southwestward along the frontal boundary was quite evident.

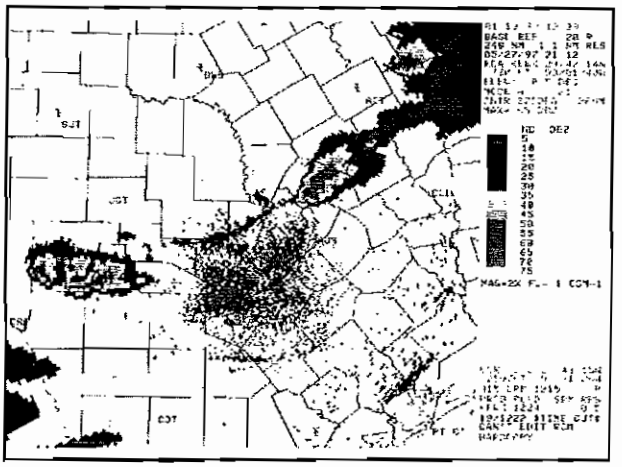

Figure 12. Williamson county storm (near center of figure) propagating southwestward along frontal boundary as seen on 2012 UTC KEWX 88D.

SRM products failed to show strong gate-to-gate shear at any elevation angle throughout the life span of this tornado. Judicial interpretation of the high resolution (.13 nm) spectrum width products aided in the location the tornado. The .54 nm spectrum width product did not resolve the tornadic feature.

Reflectivity imagery at the lowest elevation scan indicated less than 35 dBZ in the vicinity of the tornado. The overhang to the southwest was now 10-12 miles southwest of reflectivities at the lowest elevation angle as noted on reflectivity cross sections. The tornado vortex was well outside of the higher reflectivity at the 0.5 degree elevation scan. This vortex was the most difficult of the three strong tornadoes to discern using WSR-88D data even though this area was only 50 miles from the RDA site.

By 2112 UTC, an anticyclonic couplet associated with the tornadic mesocyclone over Cedar Park was located to the northeast of the mesocyclone (Fig. 13). This area of anticyclonic rotation, evident on SRM products at low to mid-elevations, was indicative of supercell storm splitting and the transition from a supercell oriented event to a mesoscale convective complex. Over the next hour the northeastern portion of the supercell would continue to split, and move southeastward away from the boundary. One hour later this clockwise rotating mass produced straight line winds of up to 80 mph across the city of Austin.

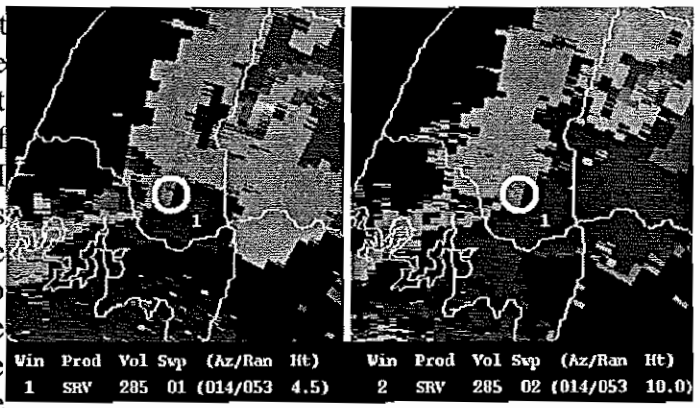

Figure 13. KEWX Storm Relative Velocity at 4.5° and 10.0° at 2112 UTC.

c. The Pedernales Valley Storm.

Between 2118 and 2135 UTC, convection continued to develop rapidly down the boundary with reflectivities aloft as much as 12 miles southwest of those at the lowest elevation angles. The evolution of the storm complex continued. Cells were developing in the lower elevations ahead (to the southwest) of the main core of the storm, providing competition for storm inflow.

Cross sections clearly show each strong updraft quickly being replaced by another to the southwest, with the complex becoming more dynamically akin to a squall line. The leading cell was approaching what appeared to be a weak boundary perpendicular to the main line of thunderstorms. Satellite and radar imagery confirmed this was a line of cumulus congestus lying in the Pedernales River Valley, formed and/or enhanced by the passage of the gravity wave hours earlier.

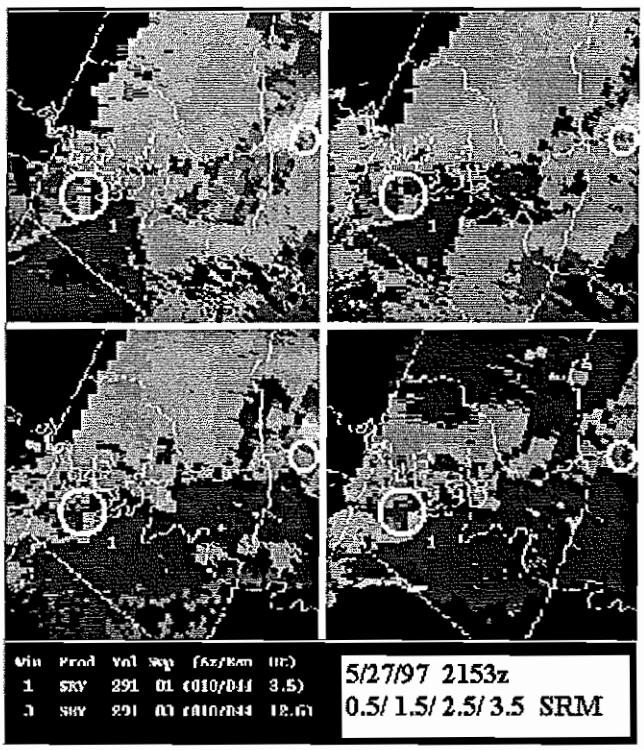

Figure 14. KEWX Storm Relative Velocity at 0.5°, 1.5°, 1.5°, 3.4° at 2153Z.

At 2141 UTC an operator-defined TVS with gate-to-gate shear of 72 kts in the lowest levels appeared and persisted through 2153 UTC (Fig. 14). A strong tornado tracked southwestward across Lake Travis for some 5 to 6 miles, 41 miles north of the RDA. The delay in obvious rotation in the lower elevations of the volume scan could have been due to low level generation of the tornado, below the 0.5 degree elevation scan.

At this time, and in subsequent volume scans, data drop out was once again occurring in the velocity products near the area of intense rotation.

Examination of the 2153 UTC 0.5 degree base reflectivity image (Fig. 15) produced the first true "hook echo" of the night from the KEWX radar. The hook was located on the "back" (northwest) side of the storm. Present at the same time were two other features on the "front side" that resembled hook echos or appendages. The feature on the back side of the storm corresponded with the location of the strong rotation depicted on the SRM product and with high spectrum width values on the 0.5 degree 0.13 nm resolution image.

Throughout the event, severe storms were occurring some 100 miles to the west along the western extent of the same surface boundary (Fig. 12). While the tornadic complex near Austin pushed to the southwest, severe storms over the Edwards Plateau and Hill Country were developing and propagating eastward. These two areas of convection merged just west of the location of the Pedernales Valley tornado. This merger ended the strong tornadic activity. The storm complex had

now fully evolved into a squall line that pushed south and southeastward producing numerous outflow boundaries and secondary lines of convection. Multiple cell and line mergers produced damaging winds across South Central Texas for several more hours, including a record 106 kt at Kelly Air Force Base in San Antonio.

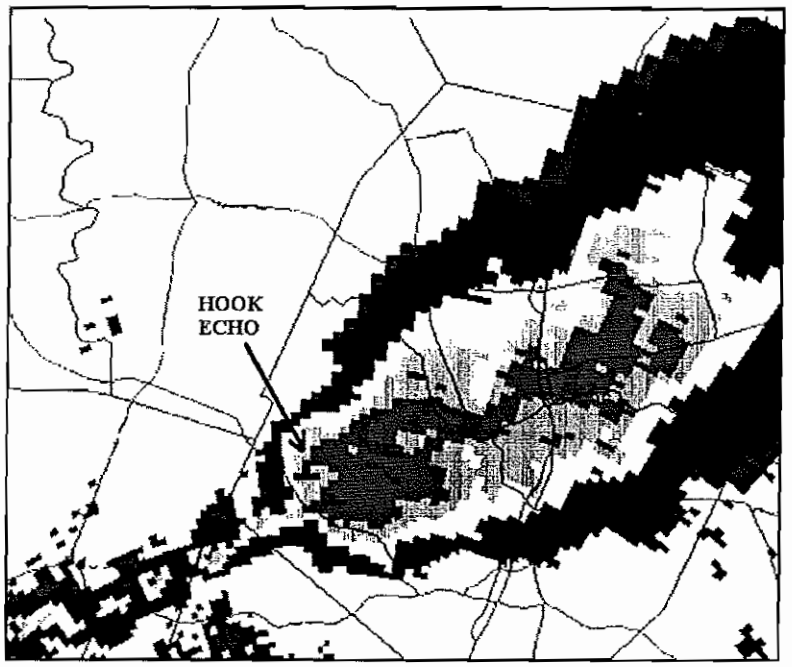

Figure 15. KEWX 0.5° Reflectivity at 2153 UTC. Hook circulation is near the end of the arrow.

5. SUMMARY DISCUSSION

The severe weather day began with weak but uninhibiting synoptic scale dynamics. A broad upper-level trough extended across the south central U.S. Extreme instability set up across much of Texas, with CAPE values over 4000 Jkg^{-1}. A weak cold front extended across central Texas, along with an inverted surface trough into south Texas. A gravity wave moved rapidly southward across central Texas from Arkansas, intersecting the cold front and extreme instability during the midday strong heating period.

Severe thunderstorms developed in the area of intersection in north central Texas and developed southwestward along the frontal boundary. The unusual movement or propagation of the storms, combined with strong low-level inflow produced helicity values and EHI values conducive for tornadic thunderstorms.

Examination of the radar imagery revealed several important factors controlling the development of severe convection. (1) The boundary was paramount in the development of tornadic activity. Isolated cells that did manage to develop off the boundary, or that moved off the boundary were short-lived and did not produce severe convection. (2) Convection developed aloft to the southwest of the core of the storm, with the overhang at times as much as 12 miles downstream. Strong

tornadoes developed from southern most cell only when no competing convection was present in the lower elevation angles. (3) Storms propagated discretely down the boundary in the early hours of the event. Actual storm movement was negligible. (4) Several hours into the event, an anticyclonic rotation which developed aloft and to the rear of the storm system in response to the extreme storm top divergence, led to splitting of the storm complex and the transition from an isolated supercell event to a squall line/MCC feature.

This event developed in a highly unusual environment, characterized by extreme CAPE with little environmental wind flow or wind shear. Only the presence of the boundary allowed the development of severe convection. As such, there were some interesting features in the radar imagery not associated traditionally with severe weather. The backward, or reverse, nature of the storms' appearance and propagation required a mental shift in interpreting the radar imagery. Storms propagated to the southwest rather than northeastward. Tornadic activity developed on the southwest leading edge, well away from any high reflectivity at the surface, and on the very leading edge of the highest reflectivities aloft. Tornadic circulations were thus consistently on the "backside" of storms. Hook echos, appendages, and strong reflectivity gradients usually associated with strong tornadoes were not present in the reflectivity imagery.

Tornadic vortices were in existence throughout much of the event and fairly long-lived land spout type vortices preceded each strong tornado. Radar imagery combined with spotter reports and videotape recordings point to three distinct tornado generating processes in the transition from weak to strong/violent tornadic activity in the three events.

The collapsing core in the center of the storm in Bell County probably played a significant part in the genesis of the F0-F1 tornados that preceded the F5 vortex at Jarrell. This genesis occurred below the level of the beam of the KEWX radar at the lowest elevation scan (7 kft). Horizontal vorticity generated along the convergent boundary by the collapse of the previous cell would have been stretched rapidly into the vertical by the highly enhanced storm inflow in the immediate vicinity of the storm. The transition of the F1 tornado to the F5 may have occurred as the maximum rotation aloft built downward as described by Trapp (Trapp, 1996) replacing the weak vortex at the surface. This process would have been accelerated and enhanced in the presence of extreme CAPE values.

There were very few clues in the radar imagery to the presence of the second strong vortex near Cedar Park, pointing to low level generation of the tornadic circulation below the existing mesocyclone. The lack of strong velocity signatures at this closer distance to the radar is puzzling.

Imagery of the third strong tornado at Pedernales Valley, while still appearing on the backside of the storm, is more typical of what is expected with tornadic activity. This vortex evolved closer to the main cell. Updrafts associated with the supercell were moving over an area of enhanced low level vorticity produced by the convection downstream (to the southwest) where the convection along the western extent of the boundary was approaching the tornadic supercells. This was the first storm in the sequence in which the existing mesocyclone could have utilized the low level vorticity generated baroclinicly by the upstream convection. The presence of enhanced cumulus in the Colorado River Valley may also have contributed to this process.

REFERENCES

Davies, Jonathan M., 1993: *Hourly Helicity, Instability, and EHI in Forecasting Supercell Tornadoes.* Preprints - 17th Conf. on Severe Local Storms, St. Louis, Missouri, Amer. Meteor. Soc., 107-111.

Davies-Jones, R. and D. Burgess, 1990: *Test of Helicity as a Tornado Forecast Parameter.* Preprints - 16th Conf. on Severe Local Storms, Kananskis Park, Alta., Canada, Amer. Meteor. Soc., 588-592.

Hart, J. A. and W. D. Korotky, 1991: *The SHARP Workstation -v1.50 A Skew T/Hodograph Analysis and Research Program for the IBM and Compatible PC User's Manual.* NOAA/NWS Forecast Office, Charleston, WV, 62.

Johns, Robert H., J. M. Davies, and P. W. Leftwich, 1993: *Some Wind and Instability Parameters Associated With Strong and Violent Tornadoes, 2. Variations in the Combinations of Wind and Instability Parameters.* The Tornado: Its Structure, Dynamics, Predictions and Hazards. Amer. Geo. Union, Washington, DC. 583-590.

Korotky, William, R.W. Przybylinski, and J. A. Hart, 1992: *The Plainfield, Illinois Tornado of August 28, 1990: The Evolution of Synoptic and Mesoscale Environments.* The Tornado: Its Structure, Dynamics, Predictions and Hazards. Amer. Geo. Union, Washington, DC. 611-624.

Trapp, J. R. and R. Davies-Jones, 1996: *The Dynamic Pipe Effect and Its Role in Tornadogenesis.* Preprints, 18th Conference on Severe Local Storms, San Francisco, California, February 1996, American Meteorological Society.

White, Andrew, Operation Support Facility, Personal Communication, September 1997.